

PAPER • OPEN ACCESS

Critical thickness of GaN on AlN: impact of growth temperature and dislocation density

To cite this article: P Sohi *et al* 2017 *Semicond. Sci. Technol.* **32** 075010

View the [article online](#) for updates and enhancements.

Related content

- [Molecular beam epitaxy for high-performance Ga-face GaN electron devices](#)
Stephen W Kaun, Man Hoi Wong, Umesh K Mishra *et al.*
- [Plasma-assisted molecular beam epitaxy of Al\(Ga\)N layers and quantum well structures for optically pumped mid-UV lasers on c-Al₂O₃](#)
S V Ivanov, D V Nechaev, A A Sitnikova *et al.*
- [Growth and applications of Group III-nitrides](#)
O Ambacher

Recent citations

- [Phase Control of Crystalline Ga₂O₃ Films by Plasma-Enhanced Atomic Layer Deposition](#)
Virginia D Wheeler *et al*
- [Coherent strain evolution at the initial growth stage of AlN on SiC\(0001\) proved by in situ synchrotron X-ray diffraction](#)
Hidetoshi Suzuki *et al*
- [Route to High Hole Mobility in GaN via Reversal of Crystal-Field Splitting](#)
Samuel Poncé *et al*



IOP | ebooks™

Bringing together innovative digital publishing with leading authors from the global scientific community.

Start exploring the collection—download the first chapter of every title for free.

Critical thickness of GaN on AlN: impact of growth temperature and dislocation density

P Sohi, D Martin and N Grandjean

Institute of Physics, École Polytechnique Fédérale de Lausanne (EPFL), CH-1015 Lausanne, Switzerland

E-mail: pirouz.sohi@epfl.ch

Received 20 February 2017, revised 1 May 2017

Accepted for publication 10 May 2017

Published 27 June 2017



CrossMark

Abstract

Critical thickness and strain relaxation of *c*-plane GaN layers grown by molecular beam epitaxy on AlN were studied as a function of growth temperature and threading dislocation density (TDD). For this purpose we used AlN/sapphire templates and AlN single crystals with TDDs of $\sim 10^9 \text{ cm}^{-2}$ and $\sim 10^3 \text{ cm}^{-2}$, respectively. Whereas at high growth temperature (900 °C) the critical thickness for plastic relaxation is only 3 monolayers (MLs) for both substrates, this value drastically increases when decreasing the growth temperature. It reaches ~ 30 MLs when GaN is deposited at 750 °C on AlN single crystals. We also observed that the strain relaxation rate strongly depends on TDD. These results exemplify the lack of efficient gliding planes in III-nitrides when grown along the *c*-axis, which, combined with low kinetics, allows for plastic relaxation to be frozen out. Achieving pseudomorphic GaN layers on AlN is of interest for two-dimensional electron gases based on AlN/GaN/AlN heterostructures lattice-matched to AlN single crystal substrates.

Keywords: AlN single crystal, critical thickness, strain relaxation, GaN, III-nitrides

(Some figures may appear in colour only in the online journal)

III-nitrides have proven to be promising materials for high power and high frequency electronic devices [1, 2]. So far, the most studied heterostructures have been AlGaIn/GaN [3] and InAlN/GaN [4, 5] grown on GaN or AlGaIn buffer layers. Despite impressive performance, III-nitride high electron mobility transistors (HEMTs) may suffer from parasitic leakage currents. One solution is to improve the carrier confinement by introducing a back-barrier with a large band offset [6]. Along these lines, a radical approach would consist in using an AlN buffer, which is a perfect electrical insulator (6.2 eV) and an excellent thermal conductor (300 W mK⁻¹). This solution could enable devices with even higher frequency and power capabilities based on AlN/GaN/AlN heterostructures with a thin GaN layer as a channel [7]. Furthermore, the recent development of AlN single crystals allows for highly strained AlN/GaN/AlN heterostructures [8, 9] that could potentially exhibit unprecedented electronic

properties thanks to the combination of a very high electron sheet carrier density, a large two-dimensional electron gas confinement, and an excellent thermal dissipation. However, one drawback of such heterostructures is the 2.4% lattice-mismatch between GaN and AlN. Consequently, strain relaxation occurs beyond a critical thickness either elastically by 2D–3D growth mode transition or plastically by dislocation generation [10]. Both phenomena affect the electron mobility due to increased scattering processes induced either by a much rougher GaN/AlN interface or by a higher dislocation density. In the past, several groups have studied the elastic strain relaxation of GaN on AlN, which is mediated by the formation of 3D islands. It is well established that such a critical thickness for the 2D–3D growth mode transition is governed by a balance between the surface energy and the elastic energy [11]. As a consequence, the critical thickness varies depending on growth conditions and/or growth techniques, with values ranging from 2 monolayers (MLs) [12] by plasma-assisted molecular beam epitaxy (PA-MBE), 4 MLs [13] by metalorganic vapor phase epitaxy, and 5 MLs [14] by NH₃-MBE. On the other hand, the onset of plastic relaxation of *c*-plane GaN on AlN has been determined to be 11–12



Original content from this work may be used under the terms of the [Creative Commons Attribution 3.0 licence](https://creativecommons.org/licenses/by/3.0/). Any further distribution of this work must maintain attribution to the author(s) and the title of the work, journal citation and DOI.

MLs [10, 15]. This exceeds by far the theoretical value of 3 MLs based on energy minimization [16] and force balance [17] models, which assume near-equilibrium growth conditions. A refined theoretical model for the description of metastable layers was proposed by Fischer *et al* [18] predicting a critical thickness of about 20 MLs. This model introduces additional terms in the force balance model by incorporating the elastic interactions between dislocations. For III-nitride materials grown along the *c*-axis, there are no proper gliding planes to ensure an efficient strain release [19], which might explain the discrepancies between theory and experimental values. Thus one should expect kinetics to have a large effect on the critical thickness.

In this study we investigate the impact of growth temperature and threading dislocation density (TDD) on the plastic relaxation of *c*-plane GaN layers grown on AlN. The critical thickness depends on the temperature and is as low as 3 MLs for near-equilibrium growth conditions. This value was obtained on AlN/sapphire template and AlN single crystal substrates, thus independent of the TDD. On the other hand, decreasing the temperature has a profound impact on the critical thickness, which increases up to 30 MLs when GaN is deposited on AlN single crystal. This exemplifies the quite inefficient relaxation scheme in GaN epilayers when grown along the *c*-axis.

The growth was performed in a Riber 21 MBE growth chamber using ammonia as nitrogen source. Conventional effusion cells were used for the evaporation of Ga and Al. For all growths NH₃ was kept at a constant flow of 200 standard cubic centimeters per minute (sccm) in order to insure N-rich growth conditions and therefore a layer by layer growth mode of GaN on AlN [10]. We used two different types of substrates: (i) commercial (Dowa) 1 μm thick AlN/sapphire templates with TDD of ~10⁹ cm⁻² and negligible residual strain¹ and (ii) commercial (HexaTech Inc.) AlN single crystals with TDD of ~10³ cm⁻². The substrate temperature was assessed using a pyrometer which measures the emission of a Mo layer evaporated on the backside of the AlN/sapphire templates. For AlN single crystals, free-carrier absorption, due to a high residual doping level was enough to heat the substrate to temperatures higher than 1000 °C. The surface temperature was then calibrated from the thermal evaporation of GaN under vacuum [20]. The growth rate was determined *in situ* either by reflection high-energy electron diffraction (RHEED) or by laser reflectometry. It varies between 0.4 and 0.5 ML s⁻¹ depending on the substrate temperature (750 °C–900 °C). Prior to the growth of GaN, the substrates were outgassed at 600 °C for 60 min. Then 100 nm of AlN was grown at 1150 °C to prepare the surface. The strain relaxation and growth mode were monitored *in situ* by RHEED with an electron gun operating at 15 kV. The RHEED pattern was recorded by a PCO Pixelfly CCD camera and a commercial software. The GaN epilayers were further characterized

¹ Negligible residual compressive strain ($\epsilon_{xx} = -0.04\%$) was found in the AlN/sapphire templates as determined by Raman spectroscopy. The measured energies for the E_2^{High} mode of AlN single crystal and AlN/sapphire template are 656.0 and 656.7 cm⁻¹, respectively.

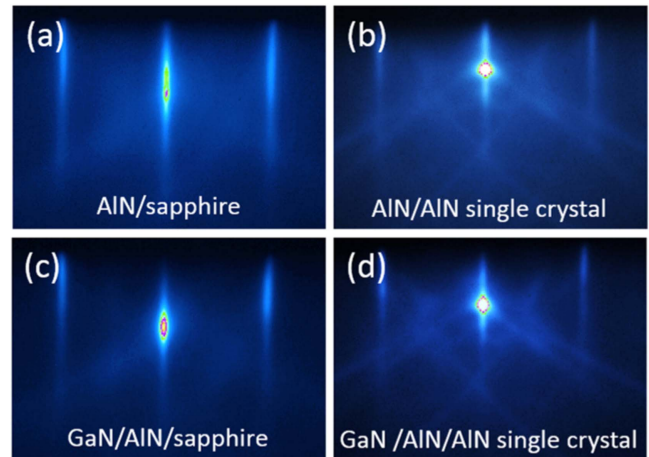


Figure 1. RHEED pattern of (a) initial AlN/sapphire and (b) AlN/AIN single crystal. After deposition of ~100 MLs of GaN at 800 °C on (c) AlN/sapphire and (d) AlN/AIN single crystal.

ex situ by high resolution x-ray diffraction (HR-XRD) using a Bruker Discovery D8 instrument system for the determination of thickness and strain by performing symmetric $2\theta-\omega$ scans along the (0002) direction. Reciprocal space mapping (RSM) was performed in some cases in order to get a deeper insight into the strain relaxation. The surface morphology was measured by atomic force microscopy (AFM).

The strain relaxation of GaN grown on AlN was measured in real-time by looking at the spacing between the (10) and ($\bar{1}0$) reflection of the RHEED pattern in the $\langle 11\bar{2}0 \rangle$ azimuth direction (figure 1). The spacing was accurately determined using a peak fitting procedure. The starting surface of AlN exhibits a streaky RHEED pattern for both substrates (figures 1(a) and (b)). Interestingly the specular beam intensity of the AlN single crystal is far more pronounced with a circular shape, indicating a very smooth surface. The RHEED pattern remains streaky during GaN growth (figures 1(c) and (d)), while the in-plane lattice parameter increases above a certain thickness. This is typical of plastic strain relaxation in contrast to elastic relaxation for which 3D islands form leading to a spotty RHEED pattern [10].

Figure 2 displays the evolution of the lattice-mismatch of GaN relative to AlN ($\Delta a/a = (a_{\text{GaN}} - a_{\text{AlN}})/a_{\text{AlN}}$), as deduced from the RHEED streak spacing, during the growth of GaN on AlN/sapphire templates for different temperatures ranging from 750 °C to 900 °C. It can be seen that the strain relaxation process strongly depends on temperature. Before further discussing the data displayed in figure 2, one should recall that the RHEED technique only probes the surface of the growing layer. Thus in order to check whether RHEED provides reliable information about the strain state within the layer, we performed *ex situ* HR-XRD measurements on several GaN layers with different thicknesses that were grown at different temperatures. The results are included in figure 2 (diamonds). A fairly good agreement is found between HR-XRD and RHEED data².

² The thermal expansion coefficients of GaN, AlN, and sapphire are similar so the cooling does not affect the strain in the GaN layer.

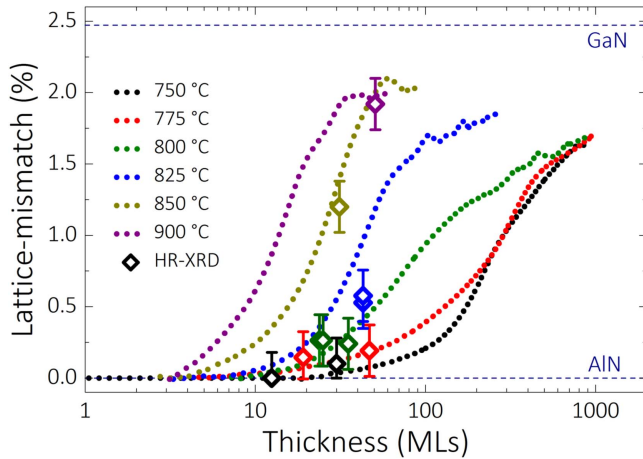


Figure 2. Evolution of the lattice-mismatch as a function of GaN layer thickness deposited on AlN/sapphire templates for substrate temperatures ranging from 750 °C to 900 °C (dotted lines). Diamonds correspond to the lattice-mismatch deduced from *ex situ* HR-XRD measurements.

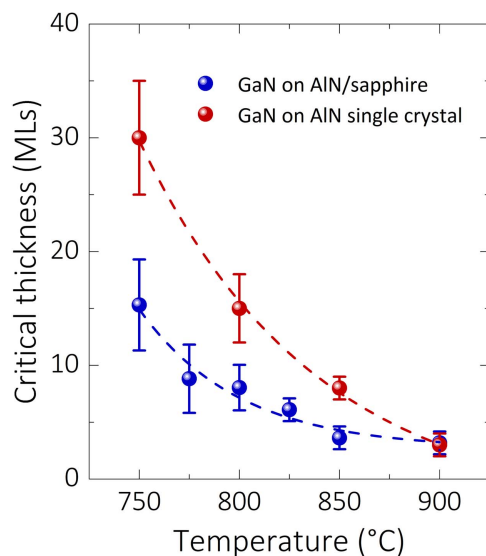


Figure 3. Critical thickness of GaN layers grown on AlN/sapphire template and AlN single crystal as a function of substrate temperature. Dashed lines are fits assuming an exponential temperature dependence (Arrhenius's law).

The main features standing out in figure 2 are the temperature dependence of the critical thickness, the strain relaxation rate, and the residual strain. This confirms the key role played by kinetics in this materials system. The dependence of the critical thickness on temperature, which is determined from the first inflection of the relaxation curves³, is presented for AlN/sapphire template and AlN single crystal substrate in figure 3. At high temperature, 900 °C, the critical thickness is 3 MLs for both substrates, which is in agreement with theoretical models developed for near-equilibrium

³ The strain relaxation curves are linearly fitted (at a fixed y-scale) and interpolated to the zero lattice-mismatch line. The critical thickness for plastic relaxation is defined as the crossing of these two lines. The uncertainty in the linear fitting of the curve leads to an error in the determination of the critical thickness, hence the error bars (in figure 3).

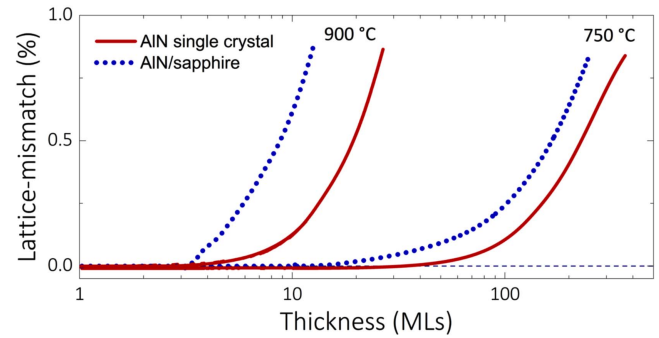


Figure 4. Comparison of strain relaxation of GaN on AlN/sapphire and AlN single crystal as a function of thickness for 750 °C and 900 °C growth temperature. The critical thickness is defined as the onset of strain relaxation.

conditions [17]. The dislocation density does not influence the critical thickness. In contrast, the critical thickness dramatically increases when decreasing the temperature. This is even more pronounced for GaN layers grown on AlN single crystal substrate for which the critical thickness reaches ~ 30 MLs for growth at 750 °C. This result is in good agreement with data reported on AlN/GaN/AlN quantum well structures on AlN single crystal grown by PA-MBE, which show a GaN pseudomorphic layer thickness of 39 MLs [8]. The lower growth temperature for GaN by PA-MBE (660 °C) likely gives rise to higher critical thickness. Note that in our case we discarded experiments performed at lower growth temperatures (< 750 °C) because the RHEED pattern became spotty, likely due to growth kinetic roughening which takes place in NH_3 -MBE.

Such a strong temperature dependence of the critical thickness has been previously observed in other material systems like Ge/Si [21], InGaAs/GaAs [22–24], MgO/Fe [25] and GaAsSb/GaAs [26]. It was shown that layers grown at low temperature are in a metastable state and fully strained, well above the calculated critical thicknesses that correspond to near-equilibrium conditions. This metastable behavior was theoretically tackled by Fischer *et al* [18] and Dodson *et al* [27] by moving away from pioneer models, which were based on force balance [17] or energy minimization [16]. Those refined models introduce kinetics by considering the interaction between dislocations. The critical thickness of GaN on AlN in the framework of the Fischer model is 20 MLs. This value should be taken with care considering that the model was proposed for Ge/Si, which has a cubic crystal structure. For wurtzite phase epilayers it has been shown using symmetry arguments that only particular slip-planes ($1/3\langle 11\bar{2}3 \rangle \{11\bar{2}2\}$ and $1/3\langle 11\bar{2}3 \rangle \{1\bar{1}01\}$) are favorable for dislocation motion [28]. This would thus lead to smaller critical thicknesses in case of III-nitrides grown along the *c*-axis.

The temperature dependence of the critical thickness and relaxation rate, versus the substrate type, i.e. the TDD, is exemplified in figure 4 for 750 °C and 900 °C. While the critical thickness is 3 MLs for both substrates at 900 °C, the early strain relaxation rate is lower in the case of the AlN single crystal. For larger thicknesses, the relaxation rates are

similar. This behavior can be understood as follows: the lack of dislocations in AlN single crystal first hinders plastic relaxation, but as the thickness increases, dislocations multiply, and eventually their density becomes high enough to allow for efficient plastic relaxation, as it does on AlN/sapphire substrate. A similar behavior is observed at 750 °C, but in this case the critical thickness is markedly different, 30 MLs and 16 MLs, for AlN single crystal and AlN/sapphire template substrate, respectively.

To get a better insight into the evolution of strain relaxation, the semi-empirical model of metastable layers proposed by Dodson and Tsao [27] was compared to our results. Within this model the driving force for strain relaxation is given by the effective stress in the layer. The relaxation process can be divided into four distinct regimes. In the first regime the growing layer accumulates elastic strain and remains pseudomorphic to the underlying substrate until the critical thickness is reached. In the second regime strain relaxation occurs via pre-existing threading dislocations (TDs) originating from the substrate. This well accounts for the different initial relaxation rates we observe right after the critical thickness is reached. In the third regime the multiplication of dislocations leads to a rapid relaxation of the strain. The mobility of such dislocations is thermally activated and is proportional to the effective stress field in the layer. This proposed mechanism well accounts for the data in figure 2 which shows different slopes as a function of temperature. Finally, in the fourth regime, when increasing further the layer thickness, the strain progressively relaxes which reduces the effective stress felt by the dislocations, therefore reducing their mobility and leading to a relaxation saturation. This explains the residual strain observed in figure 2.

The temperature dependence of the critical thickness and the strain relaxation rate should be governed by a characteristic activation energy [27, 29]. By fitting our data (dashed lines in figure 3), assuming a thermal activation (Arrhenius's law)⁴, we determine a value of 1.1 ± 0.2 and 1.6 ± 0.2 eV for GaN on AlN/sapphire and AlN single crystal substrates, respectively. Sugiura estimated the activation energy for dislocation motion in GaN to be about 2.1 eV by looking at the empirical relation between the activation energy and the band gap energy in various material groups [30]. Yonenaga *et al* experimentally determined the activation energy to be 2–2.7 eV by performing mechanical yield stress measurements [31]. Theoretical calculations performed by Holec *et al* incorporate the dislocation core into the energy minimization model and predict core energies of 1.6 eV and 3.12 eV for *a*-type (edge, $b = 1/3 \langle 11\bar{2}0 \rangle$) and (*a* + *c*)-type (mixed, $b = 1/3 \langle 11\bar{2}3 \rangle$) TDs, respectively [32]. These energies are related to the kinetic barriers created by the Peierls force that hinder the glide of dislocations [33]. The magnitude of this resistive force is large for slip systems with large Burgers vectors as for *c*-type (screw) and (*a* + *c*)-type TDs, whereas a

comparably small force for *a*-type TDs is expected, leading to a smaller activation energy. These results combined with our measurements suggest that the activation energies we determined could be possibly connected to the creation of specific types of dislocations. Further studies by transmission electron microscopy are clearly needed to clarify the actual relaxation processes.

Finally, we deposited 30 MLs of GaN at 750 °C on AlN single crystal. The HR-XRD RSM exhibits lattice matching conditions (figure 5(a)). This confirms that a rather thick (~ 8 nm) pseudomorphic GaN layer can be grown on AlN well above the near-equilibrium critical thickness of 3 MLs. The AFM image presented in figure 5(b) shows a smooth surface with a root mean square (rms) roughness of 0.4 nm over a $1 \times 1 \mu\text{m}^2$ scan. The roughness increases however slightly (0.8 nm) when looking at a larger scan ($10 \times 10 \mu\text{m}^2$) as, shown in figure 5(c). One can remark that the surface morphology is characteristic of growth in the transition regime between step-meandering and hillocks due to Ehrlich–Schwöbel barrier effects, which is typical of III-nitride layers grown at low temperatures [34]. This indicates that further work is needed to improve the surface morphology. This could be done by modifying the V/III ratio, growth rate or using In as a surfactant.

We would like to clarify that the V/III ratio does not influence the plastic strain relaxation, and thus the critical thickness, as long as the surface is smooth, i.e. large terraces of 2 MLs in height at most, which is typical for GaN grown by NH₃-MBE using N-rich conditions. On the other hand, Ga-rich conditions lead to 3D islanding which allows for elastic relaxation before dislocations are created at the island coalescence areas. This has been observed long time ago in the highly-strained InGaAs/GaAs system [35]. A similar behavior has been reported in PA-MBE for which growth may produce platelets of several MLs in height due to the low adatom mobility inherited from the strong reactivity of the nitrogen active species. Then misfit dislocations are introduced at the platelet coalescence [19]. In this case, the size and height of the platelets strongly depend on the V/III ratio, which in turn impacts the strain relaxation and thereby the critical thickness [36]. Our results are therefore valid as long as the surface morphology remains smooth, i.e. made of large terraces. This is the case for NH₃-MBE and PA-MBE for N-rich and Ga-rich conditions, respectively.

In conclusion, we studied by RHEED the strain relaxation of GaN layers grown on AlN as a function of temperature and substrates, i.e. on AlN/sapphire template and AlN single crystal. While the critical thickness is 3 MLs at 900 °C for both substrates, it increases up to 30 MLs at 750 °C when GaN is deposited on AlN single crystal. This is confirmed by performing *ex situ* HR-XRD RSM on a 30 ML thick GaN layer. The GaN layer is indeed perfectly lattice-matched. Therefore growth of GaN at low temperature on AlN single crystal enables the design of pseudomorphic AlN/GaN/AlN HEMTs with GaN channels much thicker than 3 MLs [9], which is otherwise the expected critical thickness at near-equilibrium conditions.

⁴ The mobility of dislocations is known to be thermally activated. Therefore it seems reasonable to assume as a first approximation an exponential temperature dependence of the critical thickness.

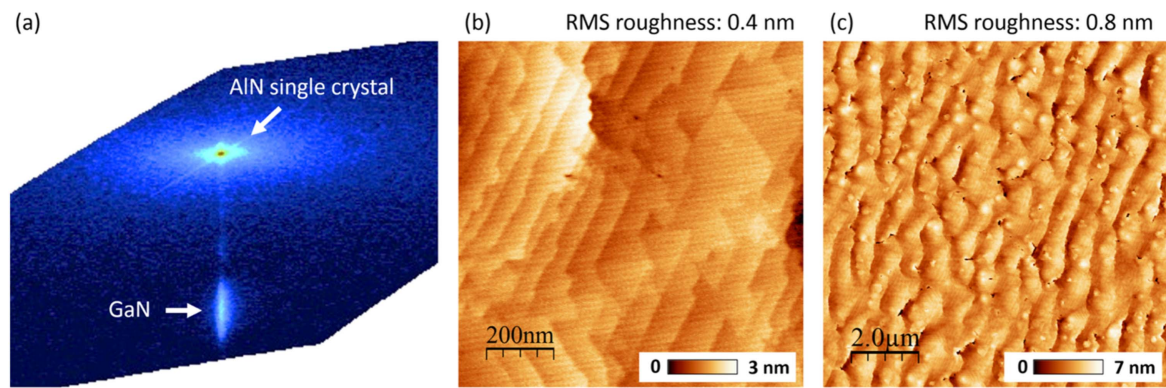


Figure 5. (a) HR-XRD RSM showing pseudomorphic GaN (30 MLs) on AlN single crystal grown at 750 °C. AFM images showing the corresponding surface morphology with RMS roughness of (b) 0.4 nm over $1 \times 1 \mu\text{m}^2$ and (c) 0.8 nm over $10 \times 10 \mu\text{m}^2$.

Acknowledgments

The present work was supported by the Swiss National Science Foundation under the grant agreement No. 200020–160049. Furthermore we would like to thank J-F Carlin, K Shojiki and S Tamariz for the reciprocal space mapping, atomic force microscopy and MBE temperature calibrations, respectively.

References

- [1] Palacios T, Chakraborty A, Rajan S, Poblencz C, Keller S, DenBaars S P, Speck J S and Mishra U K 2005 *IEEE Electron Device Lett.* **26** 781
- [2] Palacios T, Dora Y, Chakraborty A, Sanabria C, Keller S and Denbaars S P 2006 *Phys. Status Solidi a* **1850** 1845
- [3] Khan M A, Kuznia J N, Van Hove J M, Pan N and Carter J 1992 *Appl. Phys. Lett.* **60** 3027
- [4] Kuzmík J 2001 *IEEE Electron Device Lett.* **22** 510
- [5] Gonschorek M, Carlin J-F, Feltin E, Py M A and Grandjean N 2006 *Appl. Phys. Lett.* **89** 062106
- [6] Lee D S, Gao X, Guo S, Kopp D, Fay P and Palacios T 2011 *IEEE Electron Device Lett.* **32** 1525
- [7] Li G, Song B, Ganguly S, Zhu M, Wang R, Yan X, Verma J, Protasenko V, Grace Xing H and Jena D 2014 *Appl. Phys. Lett.* **104** 193506
- [8] Qi M et al 2015 *Appl. Phys. Lett.* **106** 041906
- [9] Qi M et al 2017 *Appl. Phys. Lett.* **110** 063501
- [10] Damilano B, Grandjean N, Semond F, Massies J and Leroux M 1999 *Appl. Phys. Lett.* **75** 962
- [11] Tersoff J and Tromp R M 1993 *Phys. Rev. Lett.* **70** 2782
- [12] Daudin B, Widmann F, Feuillet G, Samson Y, Arlery M and Rouvière J L 1997 *Phys. Rev. B* **56** R7069
- [13] Miyamura M, Tachibana K and Arakawa Y 2002 *Appl. Phys. Lett.* **80** 3937
- [14] Grandjean N and Massies J 1997 *Appl. Phys. Lett.* **71** 1816
- [15] Chinkyo K, Robinson I K, Jaemin M, Kyuhwan S, Myung-Cheol Y and Kyekyoon K 1996 *Appl. Phys. Lett.* **69** 2358
- [16] Frank F C and van der Merwe J H 1949 *Proc. R. Soc. A* **198** 205
- [17] Matthews J and Blakeslee A 1974 *J. Cryst. Growth* **27** 118
- [18] Fischer A, Kühne H and Richter H 1994 *Phys. Rev. Lett.* **73** 2712
- [19] Bellet-Amalric E, Adelman C, Sarigiannidou E, Rouvière J L, Feuillet G, Monroy E and Daudin B 2004 *J. Appl. Phys.* **95** 1127
- [20] Grandjean N, Massies J, Semond F, Karpov S Y and Talalaev R A 1999 *Appl. Phys. Lett.* **74** 1854
- [21] Osten H J and Klatt J 1994 *Appl. Phys. Lett.* **65** 630
- [22] Ekenstedt M J, Wang S M and Andersson T G 1991 *Appl. Phys. Lett.* **58** 854
- [23] Whaley G J and Cohen P I 1990 *Appl. Phys. Lett.* **57** 144
- [24] Kui J and Jesser W A 1991 *J. Electron. Mater.* **20** 827–31
- [25] Vassent J L, Dynna M, Marty A, Gilles B and Patrat G 1996 *J. Appl. Phys.* **80** 5727
- [26] Rodríguez B P and Millunchick J M 2006 *J. Appl. Phys.* **100** 044503
- [27] Dodson B W and Tsao J Y 1987 *Appl. Phys. Lett.* **51** 1325
- [28] Srinivasan S, Geng L, Liu R, Ponce F A, Narukawa Y and Tanaka S 2003 *Appl. Phys. Lett.* **83** 5187
- [29] Price G L 1991 *Phys. Rev. Lett.* **66** 469
- [30] Sugiura L 1997 *J. Appl. Phys.* **81** 1633
- [31] Yonenaga I, Ohno Y, Taishi T and Tokumoto Y 2009 *Physica B* **404** 4999
- [32] Holec D, Zhang Y, Rao D V S, Kappers M J, McAleese C and Humphreys C J 2008 *J. Appl. Phys.* **104** 123514
- [33] Jahnen B, Albrecht M, Dorsch W, Christiansen S, Strunk H P, Hanser D and Davis R F 1998 *MRS Internet J. Nitride Semicond. Res.* **3** 1
- [34] Kaufmann N A, Lahourcade L, Hourahine B, Martin D and Grandjean N 2016 *J. Cryst. Growth* **433** 36
- [35] Androussi Y, Lefebvre A, Delamarre C, Wang L P, Dubon A, Courboules B, Deparis C and Massies J 1995 *Appl. Phys. Lett.* **66** 3450
- [36] Bourret A, Adelman C, Daudin B, Rouvière J-L, Feuillet G and Mula G 2001 *Phys. Rev. B* **63** 245307